Transactions, **SMiRT-26**
Berlin/Potsdam, Germany, July 10-15, 2022
Division II

INSIGHTS ON HOW TO USE THE MASTER CURVE METHOD AT ELEVATED LOADING RATES

Uwe Mayer[1]

[1] Materials Testing Institute (MPA) University of Stuttgart, Germany (uwe.mayer@mpa.uni-stuttgart.de)

ABSTRACT

Some years ago a special annex for the use of the master curve method at elevated loading rates was added to ASTM E1921. The experience of several research projects, Böhme et al. (2012), Mayer (2018), using this annex provides guidance for elevated loading rate testing and the assessment of reliability of the method. Important particular characteristics of elevated loading rate tests for the test planning and evaluation are considered.

Results of fracture mechanics tests using 1T C(T) specimens at loading rates in the range of 10^5 MPa√m/s to 10^6 MPa√m/s were previously published, Mayer (2020). Recent work added results of the same material (Material 22NiMoCr3-7 from the never used Biblis C reactor pressure vessel, comparable to ASTM A508, Cl.2) and a higher strength steel (S690QL1 comparable to ASTM A514) tested in the range between 10^2 MPa√m/s and 10^4 MPa√m/s. For the lower loading rates less influence of temperature increase near the crack tip is expected. The impact of crack arrest is only dependent on the test temperature.

Test series at elevated loading rates with test temperature near to the arrest temperature do not lead to conservative results. To avoid this, choose a test temperature near the estimated reference temperature, as recommended in ASTM E1921.

INTRODUCTION

While the temperature range possible for tests at elevated loading rates using precracked Charpy specimens (PCC) according to ASTM E1820 Annex 17 is very narrow, 1 inch (1T) full size specimens according to ASTM E1820 Annex 14 can be tested in the whole range T_0 +- 50 °C. Even when ASTM E1921 recommends testing at test temperatures near to T_0 there are often reasons for the user to choose other test temperatures, for example because of limitations of the test and measurement equipment. For quasi-static tests the impact of choosing not a temperature near T_0 on precision is known. For tests at elevated loading rates there was reported an increase of deviation of the determined $T_{0,X}$ between test series at different test temperatures higher than it is expected from the measurement and statistics reasons.

There is known a connection between dynamic fracture toughness values and crack arrest. The ASME lower bound curve K_{IR} was established using both, crack arrest values and fracture toughness values at elevated loading rates. So it is not surprising, that there is an impact on the shape of the Master Curve, with decreasing difference between the elevated loading rate reference temperature$T_{0,X}$ (X = log(dK/dt)) and the crack arrest temperature $T_{KIa.}$(defined in appendix 1 of ASTM E1221), keeping in mind that the exponent of the K_{IR} lower bound curve is higher than the 0.019 / °C of the Master Curve given in ASTM E1921.

MATERIAL

Two different steel grades with were used in this project. There was material available from the forged ring of a never used reactor pressure vessel. This RPV was built for the never constructed block C of Biblis, Germany, 22NiMoCr3-7 ASTM A508, Cl.2. In previous projects was shown that this material is very homogeneous not only axial and circumferential, but also over a wide range of the thickness. Fracture mechanics specimens were extracted in T-S direction, with crack tip near ¼ resp. ¾ of the wall thickness. In a previous project quasi-static T_0 = -68 °C and RT_{NDT} = -20 °C was determined. T_{KIa} according to ASTM 1221 X1 was identical to $T_{KIa(4kN)}$ = +11°C, Mayer (2012). The other material is a higher strength steel S690QL1 comparable to ASTM A514 with RT_{NDT} = +15 °C and $T_{KIa(4kN)}$ = +12 °C. Specimens were extracted also from ¼ resp. ¾ of the wall thickness of a 200 mm thick plate.

TESTING

Fracture Mechanics Tests at Elevated Loading Rates

Dynamic testing of C(T)-specimens is specified in annex A14 of ASTM E1820. The fracture mechanics values J and K are determined basically the same way as for quasi-static tests:

$$K = \frac{F}{\sqrt{B \times B_N \times W}} \, \mathrm{f(a/w)} \tag{1}$$

$$J = J_{el} + \frac{\eta_{pl} \times A_{pl}}{B_N \times b_0} \tag{2}$$

F is the force, B the specimen thickness, B_N the specimen thickness without side grooves, W the specimen width, a the length of the crack , f(a/W) the factor calculated from a/W using equation A2.3 of ASTM E1921. J_{el} is the elastic part of the J-Integral, A_{pl} is the area under the force vs. crack opening displacement curve, b_0 the remaining ligament and $\eta_{pl} = 2 + 0.522 b_0/W$. Appropriate bandwidth and natural frequency for the measurement of force and displacement is required. It is additionally required that the inertia of the specimen does not affect the specimen compliance and the fracture mechanics values J-integral and stress intensity factor K.
In ASTM E1820 Annex A14 on Rapid load J-integral testing it is required for the time to fracture t_F that:

$$t_F > t_w \tag{3}$$

$$t_w = \frac{2\,\pi}{\sqrt{\frac{ks}{Meff}}} \tag{4}$$

The minimum test time t_W is calculated from $M_{eff,}$ the effective mass of the specimen, taken here to be half of the specimen mass and ks, the specimen-load line stiffness. For smaller test times than t_W inertial effects cannot be neglected.

Testing Device

A purpose-designed servo-hydraulic testing machine (VHS 100/20 Schenck/Instron) was used for these dynamic tests. This machine incorporates large hydraulic accumulators (2 x 280 l) and high flow rate servo-valves (6400 l/min). A special slack adapter minimizes the mass to be accelerated and hence reduces oscillations. The machine has a maximum load of 100 kN and a maximum piston displacement rate of 20 m/s. A special temperature chamber provided cooling without impeding the optical measurement. The test temperature was measured using a thermocouple attached to the specimen.

Specimen preparation

All specimens were precracked with a resonant testing machine (TESTRONIC, Rumul). The loading remains within an allowed envelope as required by ASTM E1921. The specimens had an initial crack length of $a_0/W \approx 0.52$. On both sides of each specimen 10% side grooves were machined after fatigue pre-cracking. For the calculation of fracture toughness values the exact crack length was determined after testing.

RESULTS

For the determination of the reference temperature $T_{0,X}$ according to ASTM E1921 only 6-8 fracture toughness tests are needed. Assuming the Weibull distribution with given form and a given lower limit of K_{min} = 20 MPa√m the accuracy can be calculated with a typical sigma of about 6 °C. In our projects we tested much more specimens to check, if the distribution assumed is also valid at higher loading rates. For the Biblis C material we could use results of quasi-static tests for comparison, where it was shown, that for this very homogeneous material the presumptions of ASTM E1921 were fulfilled and the accuracy was in the range expected, Roos et. al (2006). For dynamic tests there were proposals, Schindler and Kalthoff (2015), to use a different exponent p instead of 0.019 / °C for the Master Curve at higher loading rates as shown in equation 5:

$$K_{Jc(med)} = 30 + 70\, e^{p\cdot(T-T_0)} \quad (5)$$

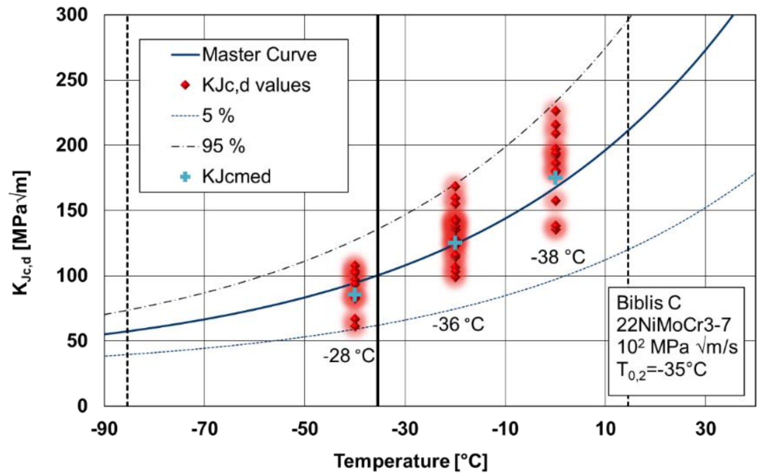

Figure 1.Fracture toughness test results for 10^2 MPa√m/s

1T C(T) specimens were tested with a loading rate of 10^2 MPa√m/s with a conventional electro-mechanical machine using clip gauges for measuring crack opening displacement (COD). The single temperature evaluation showed a decrease from the lowest to the highest test temperature of about 10 °C, figure 1.

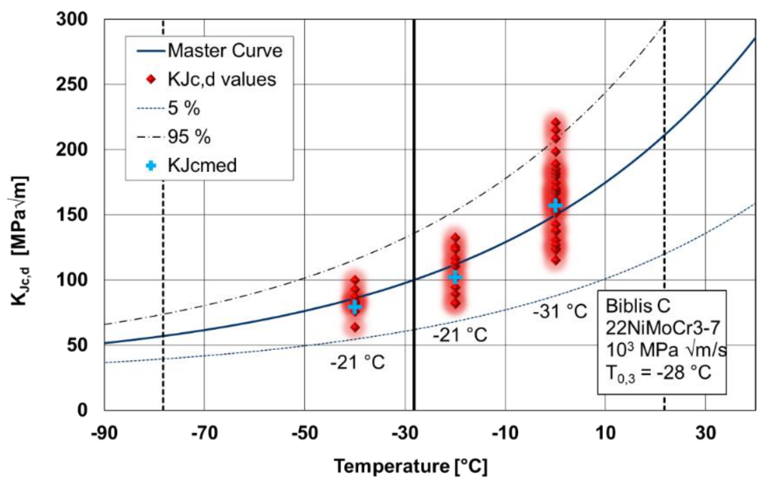

Figure 2. Fracture toughness test results for 10^3 MPa√m/s

The tests with a loading rate of 10^3 MPa√m/s were performed with the servo-hydraulic high rate testing machine and an optical measurement of the COD. There was also a 10 °C lower single temperature result for the reference temperature at the highest test temperature at 0 °C with 30 tests evaluated, figure 2.

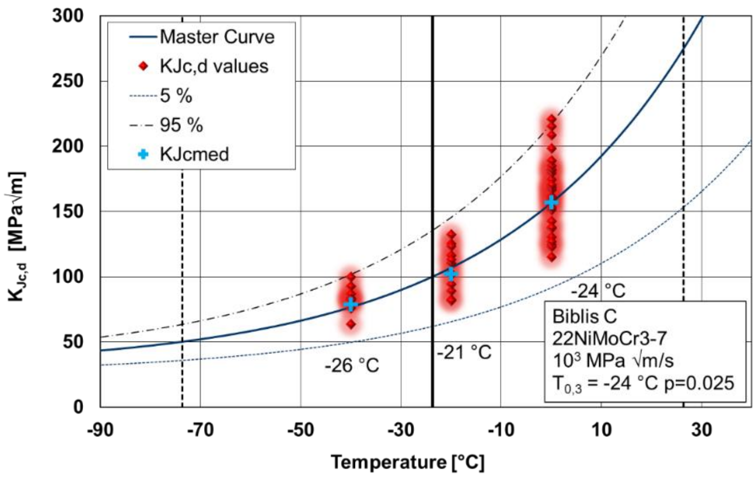

Figure 3. Fracture toughness test results for 10^3 MPa√m/s evaluated with exponent 0.025 / °C

Figures 3 and 4 show how a different exponent in the Master Curve would work for these data sets. An exponent of 0.027 / °C gives a better agreement for the single temperature evaluation at -20 °C and 0°C, but with increasing exponent the data at -40 °C fit worse in the distribution found by the total data set. This indicates that just modifying the exponent of the Master Curve is not a satisfying improvement of the procedure given in ASTM E1921, even when the experimental distribution for higher test temperature fits better in the boundaries of the Master Curve.

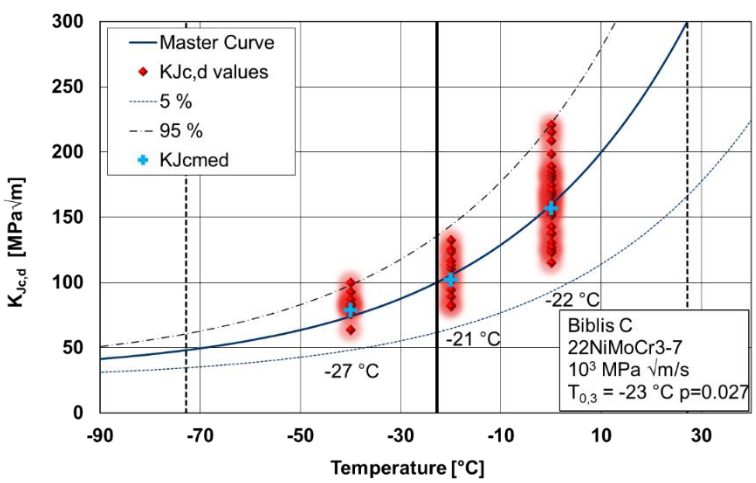

Figure 4. Fracture toughness test results for 10^3 MPa√m/s evaluated with exponent 0.027 / °C

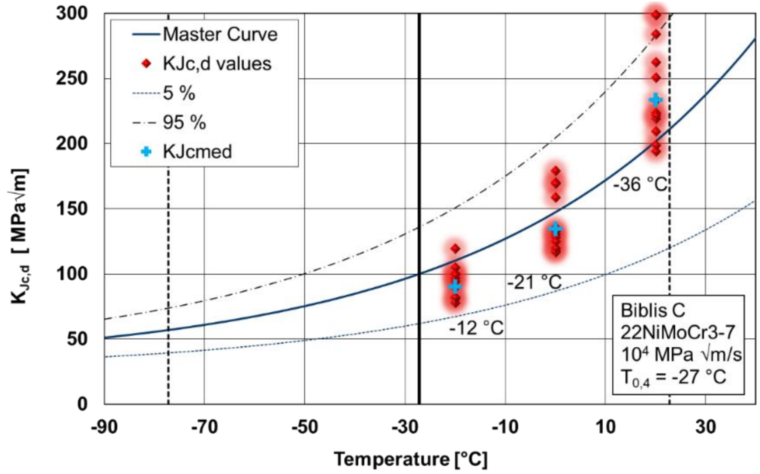

Figure 5. Fracture toughness test results for 10^4 MPa√m/s

The decrease of the single temperature results for tests with 10^4 MPa√m/s is even higher, than for the lower loading rates. Especially for the test temperature of 20 °C the resulting reference temperature $T_{0,4}$ is 24 °C lower than for the test temperature -20 °C, figure 5. Using an exponent of 0.03 / °C (figure 6) gives a better agreement of single temperature evaluation of the three test temperatures, even though there remains an obvious discrepancy between the measured distribution of the dynamic instability fracture toughness values $K_{Jc,d}$ and the expected distribution between the Master Curve boundary curves. This shows that the different behaviour of this material at testing temperatures more than 20 °C above $T_{0,X}$ cannot be described by just using another exponent for the Master Curve. For that reason we recommend strongly for a sufficient accuracy of the reference temperature $T_{0,X}$ not to rely on test results determined at test temperatures more than 20 °C higher than $T_{0,X.}$

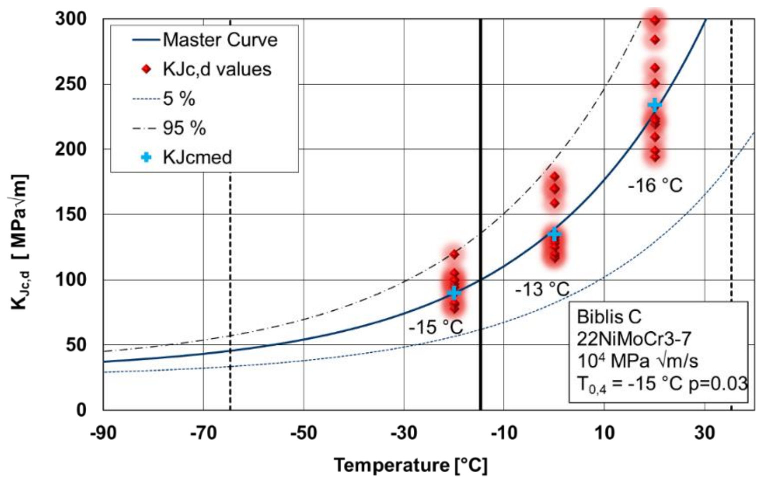

Figure 6. Fracture toughness test results for 10^4 MPa√m/s with exponent 0.03 / °C

For comparison we see two quasi-static test series, 50 1TC(T) tests each, with a much smaller difference of the single temperature reference temperature for these two test temperatures (Figure 7). Additionally the Crack Arrest Master Curve according ASTM E1221 X1, with the 90 % boundary curve is plotted.

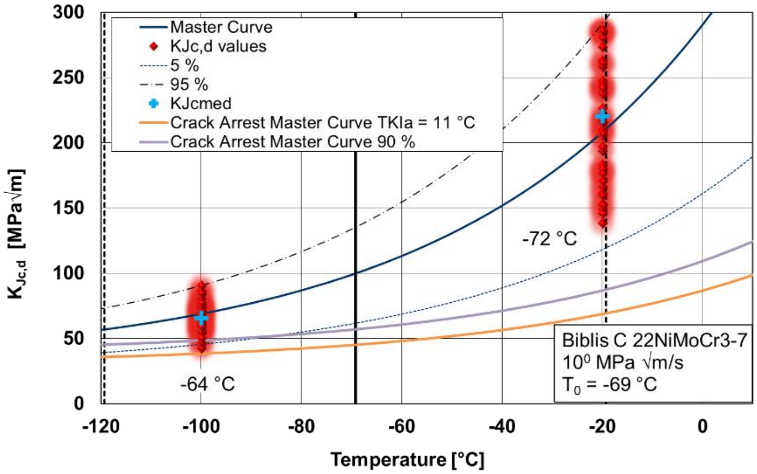

Figure 7. Quasi-static fracture toughness test results

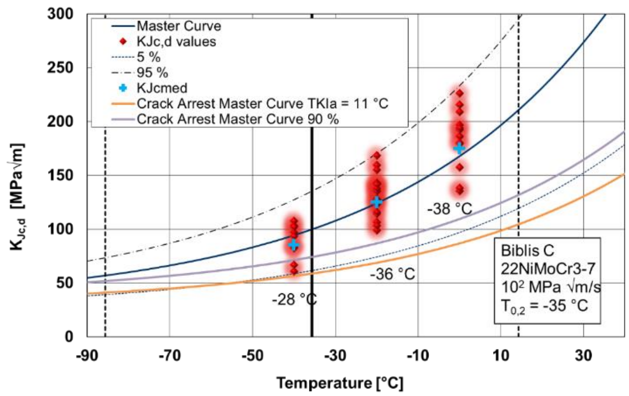

Figure 8. Fracture toughness test results for 10^2 MPa√m/s plotted with arrest curve

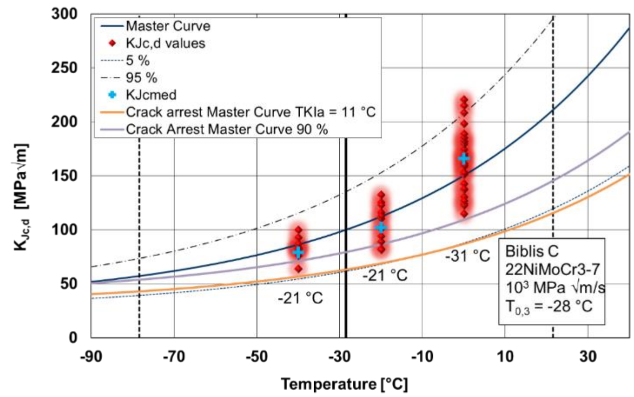

Figure 9. Fracture toughness test results for 10^3 MPa√m/s plotted with arrest curve

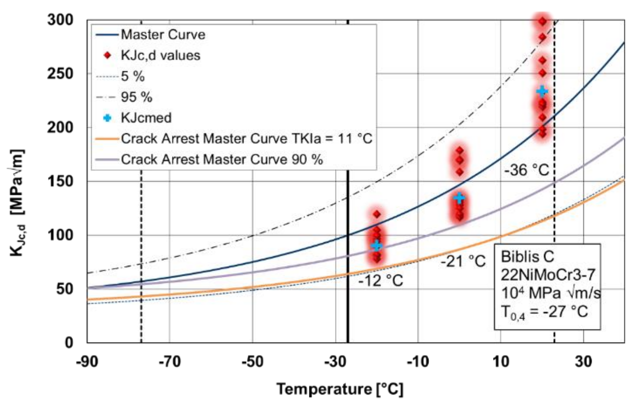

Figure 10. Fracture toughness test results for 10^4 MPa√m/s plotted with arrest curve

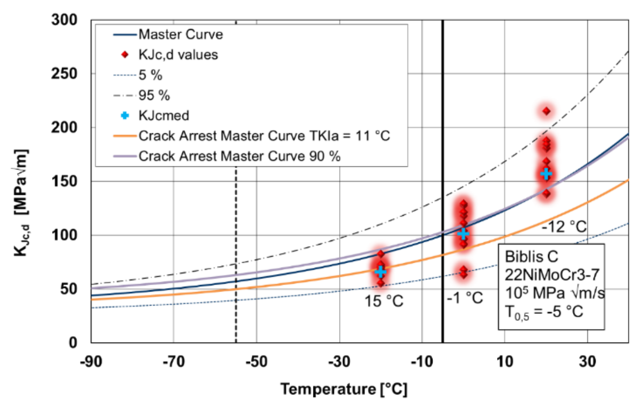

Figure 11. Fracture toughness test results for 10^5 MPa√m/s plotted with arrest curve

Fig. 8 to Fig. 11 show these curves plotted with the results for 10^2 MPa√m/s to 10^5 MPa√m/s. It is obvious that no crack arrest is expected for quasi-static tests. But for higher loading rates there is a certain probability, that after crack initiation and limited local crack growth, crack arrest occurs. A typical example of local crack arrest on the fracture surface embedded in the ductile crack growth of a specimen (L1.3BA7) tested with 10^3 MPa√m/s at 0 °C resulting in $K_{Jc,d}$ = 221 MPa is shown in figure 12 and figure 13. Crack growth direction is upwards, starting from the stretch zone. Such evidence of local crack arrest could not be found for quasi-static tests. This behaviour has an impact on the lower part of the distribution of the fracture toughness results, increasing with loading rate.

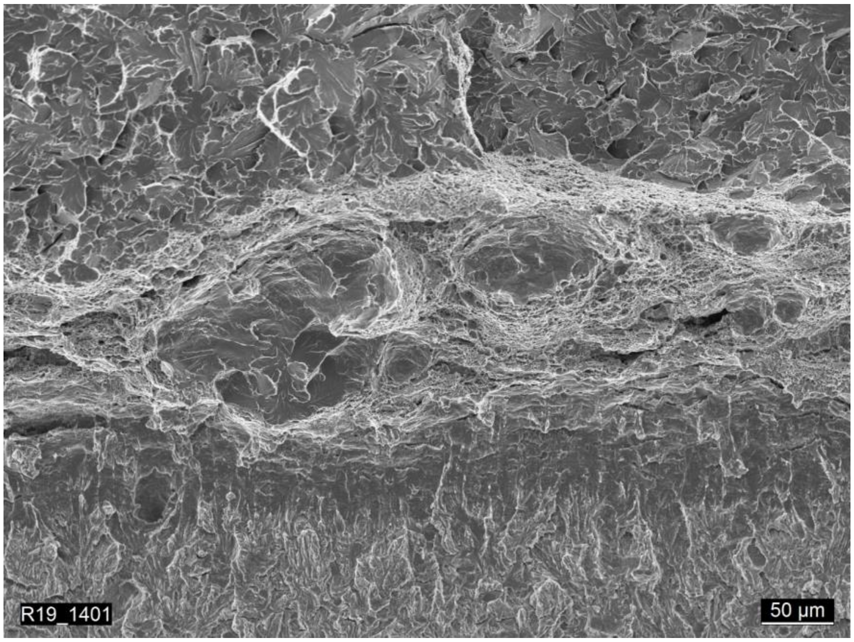

Figure 12. Fracture surface of a specimen tested with 10^3 MPa√m/s at 0°C with $K_{Jc,d}$= 221 MPa

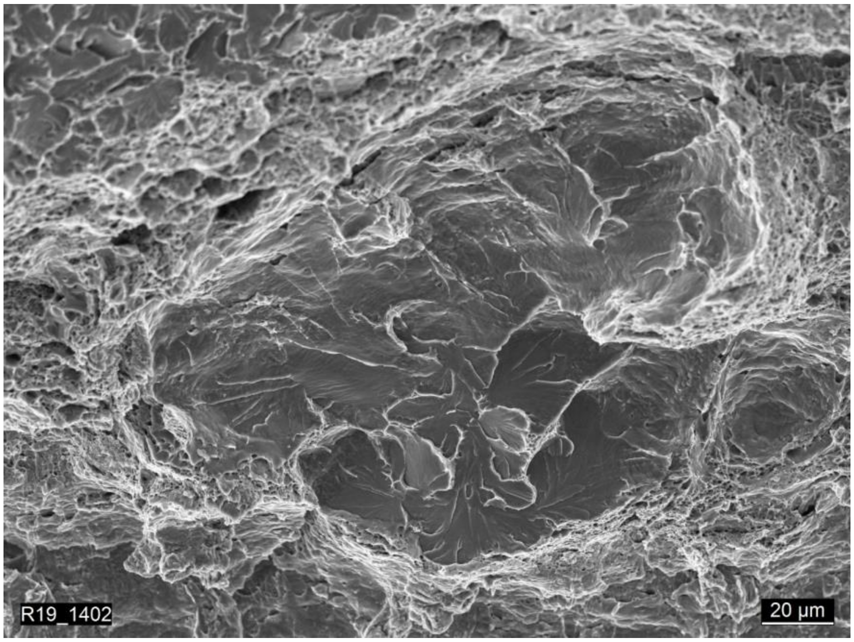

Figure 13. Detail of figure 12

We checked the transferability of these findings by testing the higher strength material S690QL1 also at the loading rates 10^3 MPa√m/s and 10^4 MPa√m/s. The quasi-static reference temperature T_0 was determined T_0 = -85 °C. There was a slight difference between the two extraction layers A and B at 1/4 and 3/4 thickness of the 200 mm thick plate, when evaluated separately yielding T_0 = -81 °C for layer A T_0 = -88 °C for layer B.

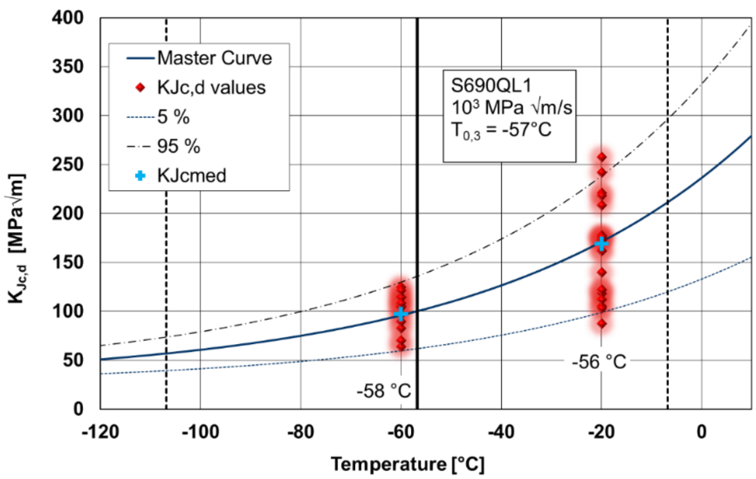

Figure 14. Fracture toughness test results for S690QL1 at 10^3 MPa√m/s

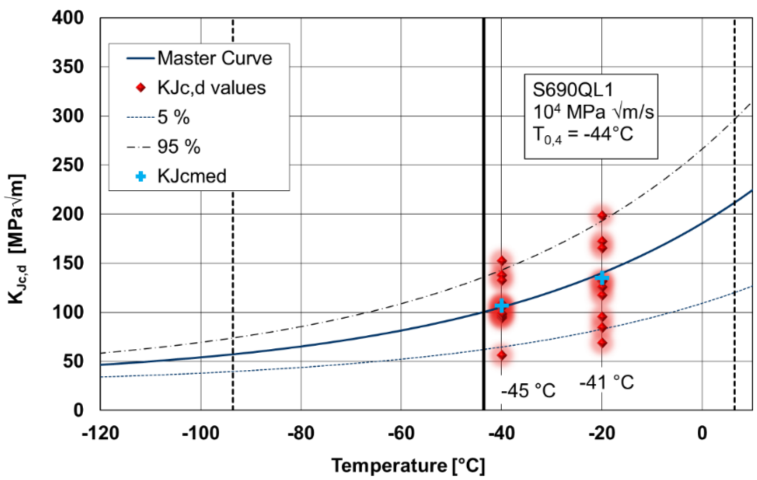

Figure 15. Fracture toughness test results for S690QL1 at 10^4 MPa√m/s

The difference of single temperature $T_{0,X}$ and multi temperature $T_{0,X}$ for the tests at loading rates 10^3 MPa√m/s (figure 14) and 10^4 MPa√m/s (figure 15) was smaller than expected from the experimental and statistical scatter for the high strength steel S690QL1. This material is tougher at lower temperature than the RPV material at the same loading rate. Still at elevated loading rates the test temperatures were below 0 °C and therefore much lower than the crack arrest temperature T_{KIa} resp. $T_{KIa(4kN)}$ (+12 °C). Figure 16 and figure 17 show that the tests at 0 °C cannot be included regarding the requirement to use only results from specimens tested in the range between T_0 - 50 °C and T_0 + 50°C. For this material the procedure of ASTM E1921 can be used for elevated loading rates without additional care for dynamic effects up to 10^4 MPa√m/s. On the fracture surface only rare occurrence of the local crack arrest phenomenon was detected, which was found very numerous for the Biblis C RPV material.

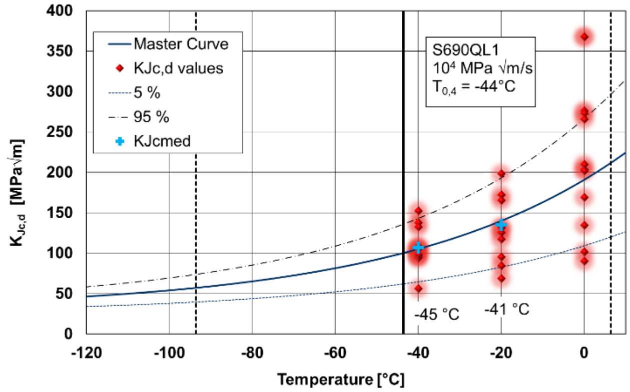

Figure 16. Fracture toughness test results for 10^4 MPa√m/s plotted with tests at 0 °C

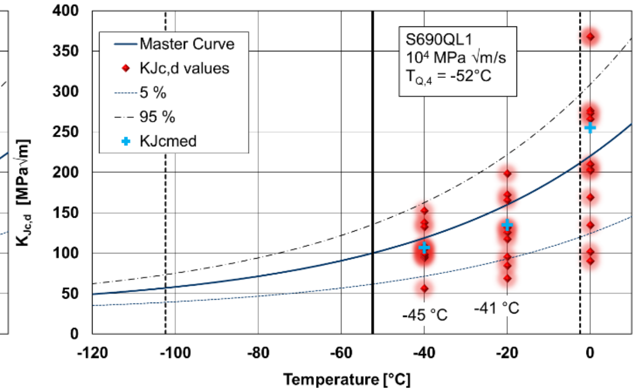

Figure 17. Evaluation of fracture test toughness results for 10^4 MPa√m/s including tests at 0 °C

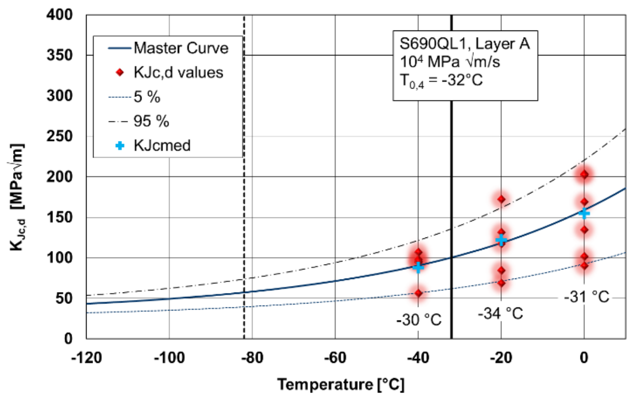

Figure 18. Fracture toughness test results for 10^4 MPa√m/s layer A

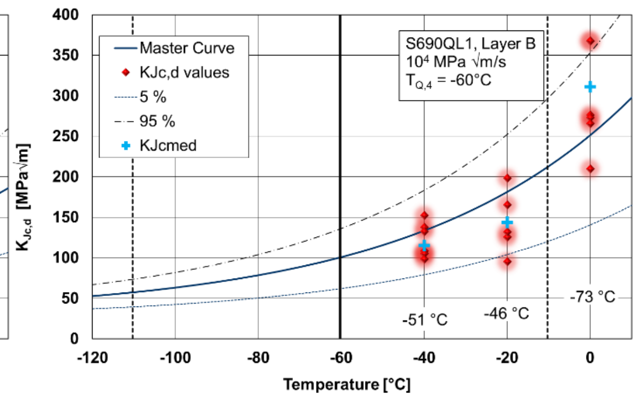

Figure 19. Fracture toughness test results for 10^4 MPa√m/s layer B

It can be seen that the difference for the reference temperature $T_{0,4}$ between the two layers A and B is higher than for the quasi-static tests. This is the reason that the test temperature 0 °C is outside the range T_0 - 50 °C and T_0 + 50°C for layer B (figure 19), while it is inside for layer A (figure 18).

CONCLUSION

Fracture mechanics test series of 1T C(T) specimens in the ductile to brittle transition region at elevated loading rates using two different materials were analyzed with regard to the impact of the choice of the test temperature on the determined reference temperature $T_{0,X}$. For the RPV material 22NiMoCr3-7, comparable to ASTM A508, Cl.2, an effect increasing with the loading rate was found yielding a lower value for $T_{0,X}$ at higher test temperatures. This was not found for the high strength steel S690QL1. This material was not as homogeneous as the RPV material.
Fracture surface investigations support the hypothesis, that the effect is pronounced for test temperatures near the crack arrest temperature. This seems to be the reason for the different sensitivity of the evaluated reference temperature $T_{0,X}$ to the choice of the test temperature, observed for the two materials. Additionally we learned from the investigations on S690QL1, that the difference in T_0 for bimodal inhomogeneity may increase with loading rate.

Instead of modifying the shape of the Master Curve the author recommends to choose the test temperature near to $T_{0,X}$ and to avoid using the full allowed range up to $T_{0,X}$ + 50 °C, which is also already mentioned in ASTM E1921 Annex 1 in clause A1.4.2.1. Otherwise the uncertainty can be significantly higher than the margin calculated in clause 10.9 of ASTM E1921.

ACKNOWLEDGMENT

The joint research project “Verification of the Master Curve Concept at Elevated Loading Rates, Subproject: Investigations using Dynamic Tests with Compact Tension Specimens.” was funded by the German Federal Ministry for Economic Affairs and Climate Action (BMWK, Project No. 1501563B) on basis of a decision by the German Bundestag.

Supported by:
Federal Ministry for Economic Affairs and Climate Action
on the basis of a decision by the German Bundestag

REFERENCES

ASTM E1820-21 (2021). “Standard Test Method for Measurement of Fracture Toughness,” *ASTM International, American Society for Testing and Materials,* West Conshohocken, PA, USA.

ASTM E1921-21a (2021). “Standard Test Method for Determination of Reference Temperature, T_0, for Ferritic Steels in the Transition Range,” *ASTM International, American Society for Testing and Materials*, West Conshohocken, PA, USA.

ASTM E1221-12a (Reapproved 2018)^{e1} (2018). “Standard Test Method for Determining Plane-Strain Crack-Arrest Fracture Toughness, K_{Ia} of Ferritic Steels,” *ASTM International, American Society for Testing and Materials*, West Conshohocken, PA, USA.

Böhme, W., Mayer, U., Reichert, T, Offermanns, S., Allmendinger, A., Hug, M., Schüler, J. and Siegele, D. (2012). “Überprüfung und Weiterentwicklung von Bewertungsmethoden für dynamische Rissinitiierung und Rissarrest, (Verification and further development of assessment methods for dynamic crack initiation and crack arrest),” *BMWi-Vorhaben* Nr. 150 1368.

Böhme, W., Reichert, T. and Mayer, U. (2013). „Assessment of dynamic fracture toughness values K_{Jc} and reference temperatures $T_{0,x}$ determined for a German RPV steel at elevated loading rates according to ASTM E1921“, published at *22nd Int. Conf. on Structural Mechanics in Reactor Technology, SMiRT-22*, San Francisco, USA.

Mayer, U. (2012). “Determination of Dynamic Fracture Toughness at High Loading Rates,” *Proceedings of the ASME 2012 International Mechanical Engineering Congress & Exposition*, IMECE2012-85383, Houston, Texas, USA, November 9-15 2012.

Mayer, U. (2018). "Verbundprojekt: Analyse und Validierung von bruchmechanischen Bewertungs-methoden für dynamische Beanspruchungen Teilprojekt: Versuche mit Kompaktzugproben und Identifikation eines Parameters für die Rissbeanspruchungsrate, (Analysis and Validation of Fracture Mechanical Assessment Methods under Dynamic Loading - Tests with Compact Tension Specimens and Identification of a Parameter for the Crack Loading Rate)", *BMWi-Vorhaben* Nr. 1501472B

Mayer, U. (2020). "Comparison between Loading Rate and Local Stress Rate When Applying ASTM E1921 at Elevated Loading Rates." *Materials Performance and Characterization* Volume 9, Issue 5, 2020.

Roos, E., Eisele, U., Lammert, R., Restemeyer, D., Schuler X. H.-P. Seebich, H.-P., Seidenfuß, M., Silcher, H. and L. Stumpfrock, L. (2006): „Kritische Überprüfung des Masterkurven-Ansatzes im Hinblick auf die Anwendung bei deutschen Kernkraftwerken“, *BMWi-Vorhaben* Nr.1501240, 2006.

Schindler, H. and Kalkhof, D. (2015): "A Closer Look at Effects of the Loading Rate on Fracture Toughness in the Ductile-to-Brittle Transition Regime of a Ferritic Steel," *Journal of Testing and Evaluation*, Vol. 43, No. 3, 2015, pp. 507-516.